

## DISCOVERY OF THE COLDEST IMAGED COMPANION OF A SUN-LIKE STAR\*

C. THALMANN<sup>1,2</sup>, J. CARSON<sup>1,3</sup>, M. JANSON<sup>4</sup>, M. GOTO<sup>1</sup>, M. MCELWAIN<sup>5</sup>, S. EGNER<sup>6</sup>, M. FELDT<sup>1</sup>, J. HASHIMOTO<sup>7</sup>, Y. HAYANO<sup>6</sup>, T. HENNING<sup>1</sup>, K. W. HODAPP<sup>8</sup>, R. KANDORI<sup>7</sup>, H. KLAHR<sup>1</sup>, T. KUDO<sup>7</sup>, N. KUSAKABE<sup>7</sup>, C. MORDASINI<sup>1</sup>, J.-I. MORINO<sup>7</sup>, H. SUTO<sup>7</sup>, R. SUZUKI<sup>6</sup>, M. TAMURA<sup>7</sup>

*Accepted for publication in ApJ Letters*

### ABSTRACT

We present the discovery of a brown dwarf or possible planet at a projected separation of  $1.9'' = 29$  AU around the star GJ 758, placing it between the separations at which substellar companions are expected to form by core accretion ( $\sim 5$  AU) or direct gravitational collapse (typically  $\gtrsim 100$  AU). The object was detected by direct imaging of its thermal glow with Subaru/HiCIAO. At 10–40 times the mass of Jupiter and a temperature of 550–640 K, GJ 758 B constitutes one of the few known T-type companions, and the coldest ever to be imaged in thermal light around a sun-like star. Its orbit is likely eccentric and of a size comparable to Pluto’s orbit, possibly as a result of gravitational scattering or outward migration. A candidate second companion is detected at  $1.2''$  at one epoch.

*Subject headings:* planetary systems — stars: low-mass, brown dwarfs — techniques: high angular resolution

### 1. INTRODUCTION

While the extrasolar planets and brown dwarf companions currently known from direct imaging mark significant discoveries, it is important to note that none of these systems present scenarios analogous to a Solar-like system. Almost all imaged substellar companions either feature extreme orbital separations (hundreds of AU, e.g. Luhman et al. 2007; Kalas et al. 2008), star-like rather than planet-like temperatures (e.g. Marois et al. 2008), or host stars at the extreme ends of the mass spectrum (A- and late M-type, e.g. Kalas et al. 2008; Chauvin et al. 2005). The closest match is probably Gl 229 B, a brown dwarf orbiting an M1 star at 40 AU (Nakajima et al. 1995). This shows how a remarkable gap still exists between recent direct-imaging discoveries and the exploration of Sun-like systems.

In this work, we present the discovery of a substellar companion with a mass of 10–40  $M_{\text{Jup}}$ , a temperature of 550–640 K, and a projected separation of  $1.9'' = 29$  AU. The estimated semi-major axis range, overlapping with our own Solar System’s outer planet orbits, along with the Sun-like parent star, make it a superior laboratory for advancing our conventional wisdom of planet or brown dwarf formation among solar-like systems.

### 2. OBSERVATIONS AND DATA REDUCTION

GJ 758 is a G9-type star, located at a distance of 15.5 pc (Gray et al. 2003; Perryman & ESA 1997). Its mass and radius are about  $0.97 M_{\odot}$  and  $0.88 R_{\odot}$ , respectively (Takeda et al. 2007). Owing to its proximity and solar-like characteristics, it has been surveyed for plane-

tary companions with the radial velocity technique (e.g. Grether & Lineweaver 2006), but no such companions have yet been reported. Furthermore, it has been studied in search of infrared excess indicating the presence of a circumstellar debris disk, but with null results (e.g. Kóspál et al. 2009).

We first detected GJ 758 B with the HiCIAO high-contrast imaging instrument (Hodapp et al. 2008) in angular differential imaging mode on Subaru telescope on May 3, 2009, with a field of view of  $20''$  and a pixel scale of 9.5 mas. The images were taken in pupil-stabilized mode in the near infrared (H band,  $1.6 \mu\text{m}$ ), where substellar objects are expected to be bright with thermal radiation (Baraffe et al. 2003; Burrows et al. 2006). The star is known to have nine field objects (Carson et al. 2009). Data reduction of the 10 exposures of 15 s revealed a hitherto unknown tenth object in close separation with  $5\sigma$  confidence. A follow-up observation of 46 exposures of 9.7 s was obtained at the next commissioning run on August 6, 2009, in which the object was successfully rediscovered with  $8.5\sigma$  confidence. The time between epochs was long enough to confirm common proper motion with GJ 758 and thus to establish a gravitationally bound system. Furthermore, the higher quality of the second observation revealed another faint signal of  $5.6\sigma$  at an even smaller separation, whose nature remains unknown until its physical existence and proper motions can be proven with a follow-up detection at a later epoch. Both runs had excellent weather conditions ( $0.5''$  natural seeing in H band).

We used a locally optimized combination of images algorithm (LOCI, Lafrenière et al. 2007a) to maximize the efficiency of the angular differential imaging technique (ADI, Marois et al. 2006). The signal-to-noise maps derived from the final images are shown in Fig. 1.

### 3. RESULTS

#### 3.1. Proper motion analysis

Located only 15.5 pc away from the Sun, GJ 758 B exhibits strong parallactic and proper motion, providing a powerful tool to distinguish physical companions to the

arXiv:0911.1127v1 [astro-ph.EP] 5 Nov 2009

\* Based on data collected at Subaru Telescope, which is operated by the National Astronomical Observatory of Japan.

<sup>1</sup> Max Planck Institute for Astronomy, Heidelberg, Germany

<sup>2</sup> E-mail: thalman@mpia.de

<sup>3</sup> College of Charleston, Charleston, South Carolina, USA.

<sup>4</sup> University of Toronto, Toronto, Canada

<sup>5</sup> Princeton University, Princeton, New Jersey, USA

<sup>6</sup> Subaru Telescope, Hilo, Hawai‘i, USA

<sup>7</sup> National Astronomical Observatory of Japan, Tokyo, Japan

<sup>8</sup> Institute for Astronomy, University of Hawai‘i, Hilo, Hawai‘i, USA

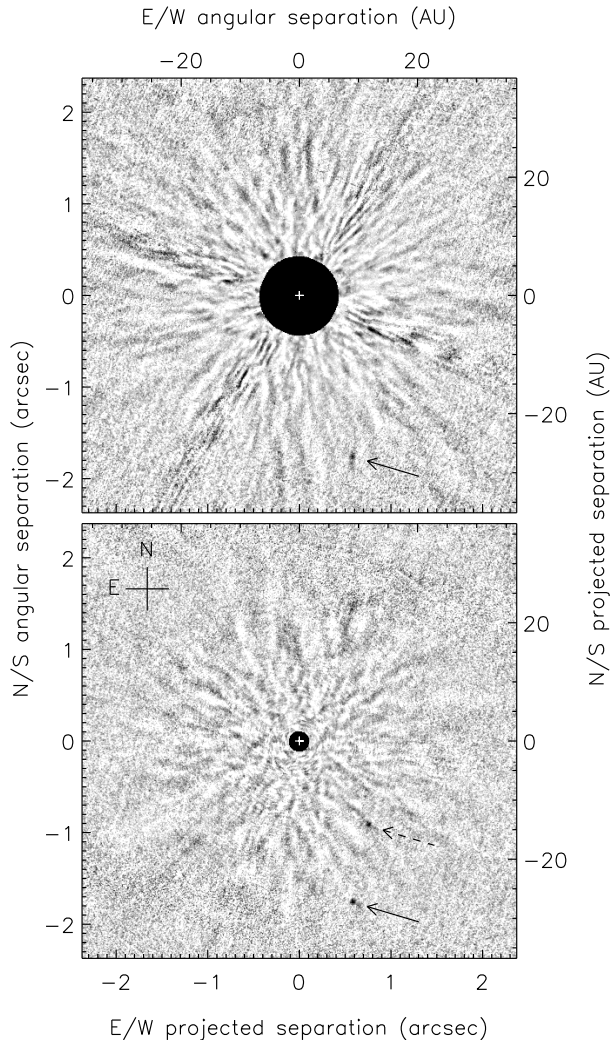


FIG. 1.— Signal-to-noise maps of the discovery images for GJ 758 B after ADI data reduction, for the May 2009 (**top**) and August 2009 (**bottom**) observations. The greyscale stretch is  $[-1\sigma, 5\sigma]$ . The S/N ratio is calculated in concentric annuli around the star. GJ 758 B is marked with solid arrows. A possible second object in the August images is pointed out with dashed arrows. The white plus sign marks the location of the host star GJ 758; the black disks designate the regions in which the field rotation arc is insufficient for ADI.

target star from unrelated background stars. In a time series of images centered on GJ 758, a companion should remain bound to its host while the background stars drift along the predicted background trajectory in unison.

Since the detections of GJ 758 B are only separated by three months, the parallactic and proper motions are of order  $0.1''$  ( $\sim 10$  HiCIAO pixels). The 7 background stars visible at both epochs were used to fine-tune the distortion correction of the images. As illustrated in Figure 2, this yields a tight cluster of proper motion vectors for the background stars, with a standard deviation on the order of the pixel scale. GJ 758 B, on the other hand, is found to share common proper motion with its host star, confirming that they form a gravitationally bound system. The companion’s observed motion deviates from the proper motion distribution of the background stars by  $10\sigma$ , thus a chance alignment can be excluded.

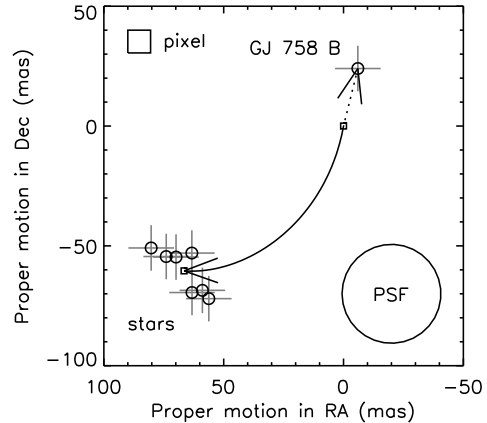


FIG. 2.— Proper motion analysis of GJ 758’s field objects. The circles show the change in the positions relative to GJ 758 in the May and August images for all 8 objects visible in both images. One-pixel error bars are drawn. The curved arrow designates the predicted parallactic and proper motion for a background star of GJ 758 between those epochs. GJ 758 B demonstrates common proper motion with its host star as well as some orbital motion (dotted arrow), whereas the other objects conform with the behavior expected from background stars. The size of the PSF resolution element and the detector pixels is provided for reference.

The precision of the distortion correction is 0.6 pixels in the central region, of the same order as the estimated precision of the centroiding of  $5\sigma$  sources. We therefore adopt a 1 pixel = 9.5 mas error bar for our astrometric measurements of GJ 758 B. The tightly constrained spread of the 7 background stars, which suffer from greater residual distortion (1.3 pixels over the whole detector) and their own proper motion (typical value 0.5 pixels in 3 months), proves this a valid assumption.

GJ 758 B is measured to move by  $(-7.6 \pm 9.5, 24.0 \pm 9.5)$  mas along the (RA, Dec) axes relative to GJ 758 between the two epochs. This represents the orbital motion of the companion around its host. No proper motion test is available for the possible second companion since it is detected only in one epoch.

### 3.2. System age

The age of the star is an important quantity to derive characteristics for the companion, including the mass and temperature. However, since GJ 758 is a field main-sequence solar-like star with no known connection to any co-moving stellar association, the age is very difficult to constrain. The isochronal analysis in Takeda et al. (2007) places the object at an age of 0.7 Gyr, with an upper limit of 3.8 Gyr at 68% confidence. The super-solar metallicity of GJ 758 ( $[\text{Fe}/\text{H}] = 0.14$  (Holmberg et al. 2009) or  $[\text{Fe}/\text{H}] = 0.22$  (Kóspál et al. 2009)) might support such a relatively young age compared to the Sun, but may also just reflect a locally metal-rich natal environment. However, the activity-rotation-age calibration in Mamajek & Hillenbrand (2008) yields an age of 6.2 Gyr given the rotational period of 39.0 days (Wright et al. 2004) and chromospheric activity  $\log R'_{\text{HK}} = -5.06$  (Duncan et al. 1991). The higher activity  $\log R'_{\text{HK}} = -4.94$  given in Wright et al. (2004) even results in 8.7 Gyr. The difference is due to monitoring during different parts of the stellar activity cycle. The discrepancy with respect to the isochronal dating could

TABLE 1  
OBSERVED QUANTITIES OF GJ 758 B AND “GJ 758 C”.

	GJ 758 B		“GJ 758 C”	
Photometry on August 6, 2009:				
App. H mag.	19.26 ± 0.16		18.47 ± 0.24	
Abs. H mag.	18.30 ± 0.16		17.51 ± 0.24	
Contrast ( $\Delta$ mag)	14.51 ± 0.16		13.72 ± 0.24	
Contrast ( $10^{-6}$ )	1.57 ± 0.18		3.24 ± 0.65	
Astrometry on May 3, 2009:				
Proj. sep. (″)	1.879 ± 0.005		—	
Proj. sep. (AU)	29.12 ± 0.08		—	
Position angle (°)	197.77 ± 0.15		—	
Astrometry on August 6, 2009:				
Proj. sep. (″)	1.858 ± 0.005		1.188 ± 0.005	
Proj. sep. (AU)	28.80 ± 0.08		18.42 ± 0.08	
Position angle (°)	198.18 ± 0.15		219.16 ± 0.08	
Assumed age (Gyr)	mass ( $M_{\text{Jup}}$ )	temp. (K)	mass ( $M_{\text{Jup}}$ )	temp. (K)
0.7	10.3	549	11.7	631
2.0	16.6	592	20.4	679
4.5	28.6	623	35.0	715
6.2	34.3	624	41.0	717
8.7	39.6	637	46.5	733

**Notes.** The conversions from flux to mass and effective temperature are based on the COND models by Baraffe et al. (2003).

possibly be explained with long-term activity cycles (e.g. Janson et al. 2008) for what concerns chromospheric activity, but the rotation is harder to explain in that context. The age from rotation alone, according to the calibration in Barnes (2007), is 5.5 Gyr.

Hence, the different age indicators for GJ 758 are discrepant. Taken together, for the purpose of our analysis, we conservatively chose the rotation-activity age estimate with the higher activity measurement of 6.2 Gyr as the baseline case for physical interpretation. For the error bars, we considered the full non-overlapping range of 0.7 to 8.7 Gyr.

### 3.3. Physical properties of GJ 758 B

The photometry of GJ 758 B and the candidate second companion are listed in Table 1. These values are based on the August 2009 data, since GJ 758 B is blended with a positive radial background structure in the May 2009 data (see Fig. 1). The mass and effective temperature are derived on the basis of the COND models by Baraffe et al. (2003) commonly used in publications on substellar companions (Marois et al. 2008; Chauvin et al. 2005). A sample of system ages is assumed, covering the range of 0.7–8.7 Gyr discussed in the target properties section.

Flux measurements were performed in flat circular apertures of 5 pixels in diameter. The loss of flux due to angular smearing in the pupil-stabilized exposures or partial subtraction in the ADI data reduction was carefully assessed and compensated.

For the baseline age of 6.2 Gyr, GJ 758 B is found to have a mass of 34.3 Jupiter masses ( $M_{\text{Jup}}$ ) and an effective temperature of 624 K. At the age of 0.7 Gyr, the mass would drop to 10.3  $M_{\text{Jup}}$ , placing the companion in the planetary regime, whereas at 8.7 Gyr it would rise to 39.6  $M_{\text{Jup}}$ , making the companion a low-mass brown dwarf. The effective temperature, on the other hand, is only weakly dependent on the system age, ranging from 549 K to 637 K. Given this effective temperature,

we expect GJ 758 B to have a T9 type spectral profile (Leggett et al. 2009). This makes GJ 758 B the coolest companion to a sun-like star ever imaged (cf.  $750 \pm 50$  K for GJ 570 D orbiting a K4 triple system at 1500 AU (Burgasser et al. 2000);  $570 \pm 25$  K for Wolf 940 B orbiting an M4 star (Burningham et al. 2009);  $810 \pm 50$  K for HD 3651 B orbiting a more sun-like K0 star (Luhman et al. 2007)). The temperature range overlaps with those of the latest-type field dwarfs (Delorme et al. 2008; Burningham et al. 2008; Warren et al. 2007), making GJ 758 B a candidate for the coldest body outside the Solar System ever thermally imaged. If the second detected object is assumed to be a real companion, its mass estimates go from 11.7  $M_{\text{Jup}}$  (also in the planetary regime) to 46.5  $M_{\text{Jup}}$  and its effective temperature from 631 K to 733 K.

All of these temperatures are low enough to allow a strong presence of methane in the atmosphere, which can be confirmed with narrow-band differential imaging in the near-infrared methane absorption bands. The current data set, taken entirely in the broadband H filter, cannot by itself exclude the possibility of a white dwarf companion in place of a brown dwarf or planet. However, the measured contrast and the maximum expected age of 8.7 Gyr render this highly unlikely. In order for the hypothetical progenitor star to live through its main-sequence lifetime, evolve into a white dwarf, and cool down to the observed H-band luminosity within 8.7 Gyr, both the lifetime of the star and the cooling timescale would have to be on the short end of the scale, implying both a high progenitor mass ( $\geq 2 M_{\odot}$ ) and a high surviving white dwarf mass ( $\sim 1.2 M_{\odot}$ ), two independently unlikely assumptions (Fontaine et al. 2001; Holberg & Bergeron 2006).

## 4. DISCUSSION

Although the relative error on the measured orbital motion of GJ 758 B is large, the data suffices to gauge the parameter space of possible orbits and derive a “best guess” set of orbital parameters. A custom Monte Carlo simulation is used for this purpose. The code generates a large number ( $10^6$ ) of orbital trajectories with random values for eccentricity  $e$ , inclination  $i$ , argument of periastron  $\omega$ , longitude of the ascending node  $\Omega$ , and a provisional semimajor axis. The distributions are presumed to be flat, except for the inclination, where larger angles are favored proportionately to  $\sin i$  in order to represent their higher geometric likelihood. The ellipse is then scaled such as to match the midpoint between the two known companion positions within the error; this sets the final value of the semimajor axis  $a$ . Next, the physical velocity vector at the midpoint is calculated for each orbit, projected into the image plane, and compared to the measured orbital motion. If it fits within the error bars, the orbital solution is considered valid, which holds for about 6% of all orbits. Finally, the ensemble of valid orbits is weighted according to the ratio of mean and current orbital velocity,  $\langle v \rangle / v_{\text{obs}}$ , to represent the statistical likelihood of finding the companion in its current position.

The results are presented in Table 2 and Figure 3. Most notably, the estimated eccentricity is very high ( $e_{\text{WM}} = 0.691$ ) and constrained. No orbital solutions below  $e < 0.25$  match the observations within the er-

TABLE 2  
ESTIMATED ORBITAL PARAMETERS OF GJ 758 B.

	Weighted median	68% likelihood
Semimajor axis $a$ (AU)	54.5	33.9–118.0
Eccentricity $e$	0.691	0.497–0.866
Inclination $i$ ( $^\circ$ )	46.5	24.0–67.4
Period $P$ (yr)	291	170–658

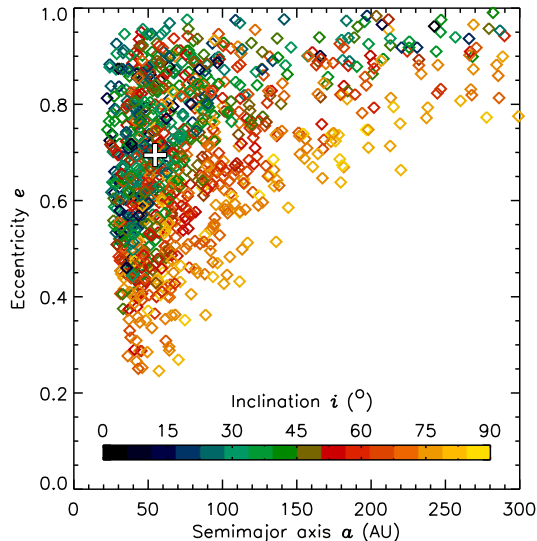


FIG. 3.— Statistical evaluation of the orbital solutions matching the observations within error bars among  $10^6$  orbits generated by a Monte Carlo simulation. The eccentricity  $e$  is plotted against the semimajor axis  $a$  for a selection of 1000 orbits biased according to statistical weight. The weight is defined as the mean orbital velocity divided by the velocity at the observed position,  $\langle v \rangle / v_{\text{obs}}$ . The orbits are color-coded to show their inclination. The weighted median value for  $(a, e)$  is marked with a white plus sign.

ror bars. The range of semimajor axes (33.9–118.0 AU) places the companion in the brown dwarf desert.

The orbital separation is too large to be the result of *in situ* formation by core accretion (Mordasini et al. 2008; Dodson-Robinson et al. 2009). Likewise, while gravitational instability (Boss 2003) may in principle occur at these ranges (Foltin & Klahr 2009, in prep.), simulations by Stamatellos & Whitworth (2009) suggest that such objects either rapidly grow into full-fledged stars or are scattered to larger separations. This leaves the possibility of formation by core accretion and subsequent outward transport by either gravitational scattering (Veras et al. 2009) or outward migration as part of a resonant pair of companions sharing a common disk gap (Crida et al. 2009).

Scattering typically leaves companions in eccentric orbits, which matches the observation. On the other hand, should GJ 758 C turn out to be a real companion orbiting

inwards from GJ 758 B, its separation would be too large to be the scattering partner. Conversely, it would fit the pair-wise migration scenario particularly well, especially since it would be more massive than GJ 758 B, as the mechanism requires. At any rate, such a configuration would likely be unstable on long timescales, favoring a young system with planet-mass companions.

Finally, GJ 758 B could already have formed during the star formation phase, as a result of fragmentation of the molecular cloud (e.g. Bate et al. 2002), making it a “failed star”. However, such brown dwarfs are generally ejected from the stellar system due to interactions with other, more massive members of the forming cluster, or undergo further accretion to become a full-fledged star. The resulting scarcity of brown dwarfs in orbit around stars (conservative upper limit of 4% in Lafrenière et al. 2007b) is known as the brown dwarf desert. Accordingly, the hydrodynamic simulations of Bate & Bonnell (2005) favor the formation of close binaries (<10 AU) roughly equal-mass components; the few wide binaries with mass ratios <0.25 are formed by chance combination of two stars ejected from the cluster at the same time. Since a  $0.97 M_{\odot}$  star like GJ 758 belongs to the most massive members of its birth cluster, it is unlikely to undergo ejection and therefore does not fit this scenario.

## 5. CONCLUSIONS

We present the discovery of a substellar companion to the star GJ 758 at a separation of  $1.9''$  by angular differential imaging in H-band with Subaru/HiCIAO. Common proper motion with its host is demonstrated. We derive ranges of  $10.3\text{--}39.6 M_{\text{Jup}}$  for the mass and  $549\text{--}637\text{ K}$  for the temperature of the companion, classifying it as either a methane-bearing high-mass planet or low-mass brown dwarf. A candidate second companion is detected at a separation of  $1.2''$ , which could represent a migration partner of GJ 758 B.

This unique configuration of the GJ 758 system, its short dynamical timescale (observable motion in only 3 months), and its demonstrated accessibility by angular differential imaging, make it an excellent showcase target for the direct investigation of the formation and evolution mechanisms of planets and brown dwarfs.

We thank David Lafrenière for generously providing us with the source code for his LOCI algorithm, and the Subaru AO188 commissioning team for enabling and supporting our ADI-mode observations. This work is partly supported by a Grant-in-Aid for Science Research in a Priority Area from MEXT, Japan, and the U.S. National Science Foundation under Award No. AST-0901967. This publication makes use of the SIMBAD and NStED databases.

*Facilities:* Subaru (HiCIAO, AO188)

## REFERENCES

- Baraffe, I., Chabrier, G., Barman, T. S., Allard, F., & Hauschildt, P. H. 2003, *A&A*, 402, 701  
 Barnes, S. A. 2007, *ApJ*, 669, 1167  
 Bate, M. R., Bonnell, I. A., & Bromm, V. 2002, *MNRAS*, 336, 705  
 Bate, M. R., & Bonnell, I. A. 2005, *MNRAS*, 356, 1201  
 Biller, B. A., Kasper, M., Close, L. M., Brandner, W., & Kellner, S. 2006, *ApJ*, 641, L141  
 Boss, A. P. 2003, *ApJ*, 599, 577  
 Burgasser, A. J., et al. 2000, *ApJ*, 531, L57  
 Burningham, B., et al. 2008, *MNRAS*, 391, 320  
 Burningham, B., et al. 2009, *MNRAS*, 395, 1237  
 Burrows, A., Sudarsky, D., & Hubeny, I. 2006, *ApJ*, 640, 1063  
 Carson, J. C., Hiner, K. D., Villar, G. G., Blaschak, M. G., Rudolph, A. L., & Stapelfeldt, K. R. 2009, *AJ*, 137, 218

- Chauvin, G., et al. 2005, *A&A*, 438, L29
- Crida, A., Masset, F., & Morbidelli, A. 2009, arXiv:0910.1004
- Delorme, P., et al. 2008, *A&A*, 482, 961
- Dodson-Robinson, S. E., Veras, D., Ford, E. B., & Beichman, C. A. 2009, arXiv:0909.2662
- Duncan, D. K., et al. 1991, *ApJS*, 76, 383
- Foltin, D. & Klahr, H. 2009, in prep.
- Fontaine, G., Brassard, P., & Bergeron, P. 2001, *PASP*, 113, 409
- Gray, R. O., Corbally, C. J., Garrison, R. F., McFadden, M. T., & Robinson, P. E. 2003, *AJ*, 126, 2048
- Grether, D., & Lineweaver, C. H. 2006, *ApJ*, 640, 1051
- Hodapp, K. W., et al. 2008, *Proc. SPIE*, 7014,
- Holberg, J. B., & Bergeron, P. 2006, *AJ*, 132, 1221
- Holmberg, J., Nordström, B., & Andersen, J. 2009, *A&A*, 501, 941
- Janson, M., Reffert, S., Brandner, W., Henning, T., Lenzen, R., & Hippler, S. 2008, *A&A*, 488, 771
- Kalas, P., et al. 2008, *Science*, 322, 1345
- Kóspál, Á., Ardila, D. R., Moór, A., & Ábrahám, P. 2009, *ApJ*, 700, L73
- Lafrenière, D., Marois, C., Doyon, R., Nadeau, D., & Artigau, É. 2007a, *ApJ*, 660, 770
- Lafrenière, D., et al. 2007b, *ApJ*, 670, 1367
- Leggett, S. K., et al. 2009, *ApJ*, 695, 1517
- Luhman, K. L., et al. 2007, *ApJ*, 654, 570
- Mamajek, E. E., & Hillenbrand, L. A. 2008, *ApJ*, 687, 1264
- Marengo, M., Stapelfeldt, K., Werner, M. W., Hora, J. L., Fazio, G. G., Schuster, M. T., Carson, J. C., & Megeath, S. T. 2009, *ApJ*, 700, 1647
- Marois, C., Lafrenière, D., Doyon, R., Macintosh, B., & Nadeau, D. 2006, *ApJ*, 641, 556
- Marois, C., Macintosh, B., Barman, T., Zuckerman, B., Song, I., Patience, J., Lafrenière, D., & Doyon, R. 2008, *Science*, 322, 1348
- Mordasini, C., Alibert, Y., Benz, W., & Naef, D. 2008, *Astronomical Society of the Pacific Conference Series*, 398, 235
- Nakajima, T., Oppenheimer, B. R., Kulkarni, S. R., Golimowski, D. A., Matthews, K., & Durrance, S. T. 1995, *Nature*, 378, 463
- Perryman, M. A. C., & ESA 1997, *ESA Special Publication*, 1200
- Scholz, R.-D., McCaughrean, M. J., Lodieu, N., & Kuhlbrodt, B. 2003, *A&A*, 398, L29
- Stamatellos, D., & Whitworth, A. P. 2009, *MNRAS*, 392, 413
- Takeda, G., Ford, E. B., Sills, A., Rasio, F. A., Fischer, D. A., & Valenti, J. A. 2007, *ApJS*, 168, 297
- Veras, D., Crepp, J. R., & Ford, E. B. 2009, *ApJ*, 696, 1600
- Warren, S. J., et al. 2007, *MNRAS*, 381, 1400
- Wright, J. T., Marcy, G. W., Butler, R. P., & Vogt, S. S. 2004, *ApJS*, 152, 261